JOURNAL OF GEOPHYSICAL RESEARCH, VOL. 92, NO. B6, PAGES 4853–4866, MAY 10, 1987

Olivine-Spinel Transitions: Experimental and Thermodynamic Constraints and Implications for the Nature of the 400-km Seismic Discontinuity

CRAIG R. BINA AND BERNARD J. WOOD

Department of Geological Sciences, Northwestern University, Evanston, Illinois

The sequence of high-pressure phase transitions $\alpha \rightarrow \beta \rightarrow \gamma$ in olivine is traditionally used as a model for seismic velocity variations in the 200- to 650-km-depth interval in a mantle of peridotitic bulk composition. It has been proposed that the observed seismic velocity increase at 400-km depth is too sharp and of too small a magnitude to be attributable to the $\alpha \rightarrow \beta$ phase change and that the upper mantle must thus be chemically stratified, with the 400-km discontinuity being due either to a combination of phase changes in a layer of pyroxene/garnet-rich "piclogite" composition or to a chemical boundary between such a piclogite layer and an overlying peridotitic layer. Using available calorimetric, thermoelastic, and synthesis data (and their associated experimental uncertainties), we have derived internally consistent high-pressure phase relations for the Mg_2SiO_4-Fe_2SiO_4 join. We find that the divariant transition $\alpha \rightarrow \alpha+\beta \rightarrow \beta$, which is generally regarded as occurring over a broad depth interval for mantle olivine compositions, is, in fact, extremely sharp. The seismic discontinuity corresponding to the $\alpha \rightarrow \alpha+\beta \rightarrow \beta$ transition in $(Mg_{0.9}Fe_{0.1})_2SiO_4$ should occur over a depth interval (isothermal) of about 6 km at a depth of approximately 400 km; the sharpness of this transition is quite insensitive to uncertainties in the constraining calorimetric, thermoelastic, and synthesis data. In addition, we have computed seismic velocity profiles for a model mantle consisting of pure olivine of $(Mg_{0.9}Fe_{0.1})_2SiO_4$ composition. Comparison of these computed profiles to those derived from recent seismic studies indicates that the magnitude of the observed velocity increase at 400-km depth is consistent with a mantle transition zone composed of about 60-70% olivine. We conclude that there is no need to infer the existence of pyroxene/garnet-rich compositions, such as eclogite or "piclogite," in the transition zone, since an upper mantle of homogeneous olivine-rich peridotitic composition is consistent with the available seismic velocity data.

INTRODUCTION

The abrupt increase in seismic velocity at approximately 400-km depth is indicative of a change in the elastic properties of the materials comprising the earth's upper mantle. This change has been ascribed to a phase transformation in one of the major mineralogic constituents of the mantle [e.g., *Ringwood*, 1970]. Samples of the upper mantle occur as xenoliths in kimberlites and in alkalic basalts [*Ringwood*, 1975] and are generally of peridotitic (olivine-rich) or eclogitic (clinopyroxene-plus-garnet) mineralogy. *Bernal* [1936] proposed that the velocity increases in the transition zone were produced by the transformation of olivine to the spinel structure. His suggestion has been reiterated and amplified with recent high-pressure experimental data [e.g., *Akimoto and Fujisawa*, 1968, *Ringwood and Major*, 1970; *Kawada*, 1977; *Suito*, 1977]. These authors have shown that a transformation of α-$(Mg,Fe)_2SiO_4$ (olivine) to either γ-$(Mg,Fe)_2SiO_4$ (spinel structure) or to β-$(Mg,Fe)_2SiO_4$ (modified spinel) would produce a significant change in density and seismic velocities at approximately 400-km depth for a mantle of peridotitic composition. Despite the wide acceptance of the peridotitic model for the upper mantle [*Ringwood*, 1975, *Liu*, 1979, *Jeanloz and Thompson*, 1983; *Navrotsky and Akaogi*, 1984; *Weidner*, 1985], it has been suggested [*Bass and Anderson*, 1984; *Anderson and Bass*, 1986] that a phase change in olivine would give rise to a gradual increase in seismic velocity over a considerable depth interval, rather than the observed abrupt increase, and that the magnitude of the velocity increase due to such a transition would be more than twice that actually observed seismically. These authors state that the seismic data indicate that the transition zone is chemically distinct from the uppermost mantle, with the transition zone composed of a pyroxene/garnet-rich "piclogite" layer containing 16% [*Bass and Anderson*, 1984] or 30% [*Anderson and Bass*, 1986] olivine. They thus ascribe the 400-km discontinuity to either a chemical boundary between the piclogite layer and the overlying peridotite or, if this boundary is referred to a shallower depth, to a phase change in the eclogitic and olivine components of the piclogite. The nature of the 400-km discontinuity has important geologic implications; a chemical discontinuity could inhibit convection, producing a thermal boundary layer and isolating the mantle into distinct geochemical reservoirs [cf. *Christensen and Yuen*, 1984].

Isochemical phase transformations are, in general, difficult to reconcile with sharp seismic discontinuities. This is because phase transitions in complex multicomponent systems are generally multivariant in nature and so give rise to smooth gradients in seismic velocity over broad depth intervals, as shown in Figure 1. A viable phase transition model for the 400-km discontinuity must be exceptional in that it must be nearly univariant (Figure 1). In a previous study [*Bina and Wood*, 1984] we demonstrated that the major mineralogic transformation in eclogite at about 400-km depth, pyroxene dissolving into garnet (majorite), is multivariant and would not produce an appropriate seismic discontinuity (Figure 1). The major purpose of this study has been to determine whether or not a phase transformation in the Mg_2SiO_4-Fe_2SiO_4 system could produce, under isochemical conditions, a sharp seismic discontinuity. We therefore follow *Navrotsky and Akaogi* [1984] and *Weidner* [1985] in examining the main

Paper number 6B6027.
0148-0227/87/006B-6027$05.00

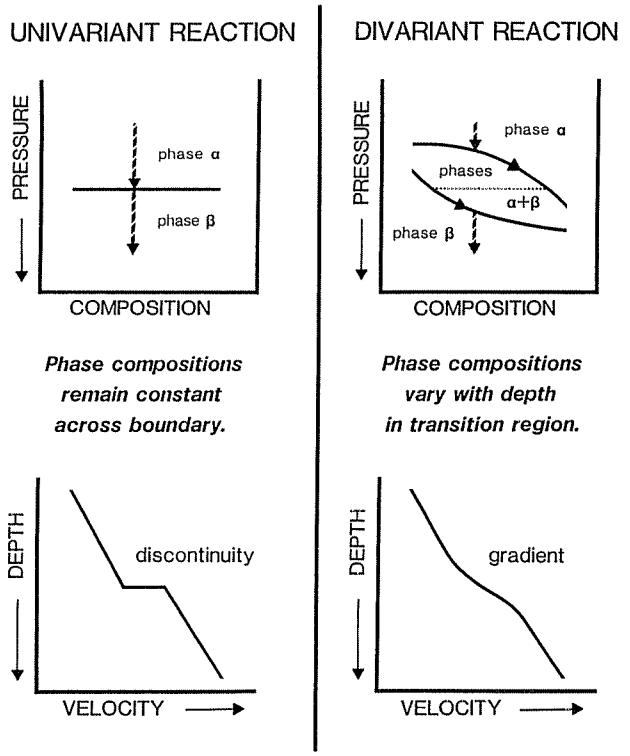

Fig. 1. In simple systems, univariant reactions occur in which a phase α of fixed composition transforms directly into a phase β of fixed composition, giving rise to a sharp discontinuity in material properties (e.g., seismic velocities) at a given depth. In complex systems, divariant reactions occur in which a phase α transforms to a phase β via an intervening region (an "$\alpha+\beta$ loop") in which both phases are stable and in which the distribution and compositions of the two phases vary continuously; this gives rise to a smooth, continuous gradient in material properties (e.g., seismic velocities) over a finite depth interval.

phase transformations to be expected in peridotitic compositions, namely, α-$(Mg,Fe)_2SiO_4 \rightarrow$ β-$(Mg,Fe)_2SiO_4 \rightarrow$ γ-$(Mg,Fe)_2SiO_4$.

Navrotsky and Akaogi [1984] used available high-pressure experimental data together with 1 atm calorimetric measurements and volumes to produce an internally consistent model of the Mg_2SiO_4-Fe_2SiO_4 phase diagram at high pressures and temperatures. Although they found that the $\alpha+\beta$ divariant loop was quite narrow (about 10 km wide), these authors' calculated phase diagram generates a smeared out discontinuity at 400 km because at probable mantle temperatures and compositions (Mg/(Mg+Fe)~0.9), the α phase breaks down to $\alpha+\gamma$ (with small amounts of γ) before the β phase appears. Their results, which provide a basis for our work, may be refined in two important ways. First, *Navrotsky and Akaogi* [1984] took no account of the compressibilities and coefficients of thermal expansion of the α, β, and γ phases and hence assumed the volume changes of reaction to be independent of pressure and temperature. This is a substantial oversimplification because the bulk modulus of the α phase is much less than that of the β and γ phases [*Weidner et al.*, 1984], and incorporation of these data alters the calculated phase relations appreciably. (For example, the calculated free energy difference between the α and β phases of Mg_2SiO_4 component at 1000°C and 100 kbar increases by more than 600 cal (about 10%) upon inclusion of the pressure and temperature dependence of the volumes.) Second, *Navrotsky and Akaogi* [1984] assumed that the Mg and Fe atoms mix ideally in all three phases, an assumption which, although a reasonable first approximation, is not strictly correct [*Wood and Kleppa*, 1981]. In this study we have made use of all the available thermodynamic, thermoelastic, and high-pressure experimental data for the olivine polymorph phases. We have used these data to compute internally consistent phase diagrams for the Mg_2SiO_4-Fe_2SiO_4 join and to calculate density and seismic velocity profiles as functions of pressure and temperature for a model mantle of pure olivine $(Mg_{0.9}Fe_{0.1})_2SiO_4$ composition.

METHOD OF APPROACH

The phase diagram for olivine in pressure-composition space is usually drawn as shown in Figure 2. The $\alpha+\beta$ divariant field is generally sketched as a broad loop, hence olivine with a presumed mantle Mg/(Mg+Fe) ratio (~0.9) would undergo a gradual transition from the α to the β phase with increasing pressure, giving rise to a smooth variation in elastic properties and seismic velocities over a broad depth interval (Figure 1). However, as also shown in Figure 2, the width of the $\alpha+\beta$ loop is not well constrained by the high-pressure data since no experiments have, to date, produced an equilibrium $\alpha+\beta$ phase assemblage in mantle olivine compositions. In order to determine the nature of the $\alpha \rightarrow \alpha+\beta \rightarrow \beta$ transition, it is necessary to use other types of experimental data. These data enable us to compute an olivine phase diagram which is internally consistent thermodynamically and in which the width of the $\alpha+\beta$ divariant loop is well constrained.

In order to calculate a phase diagram, it is necessary to have enthalpy (H_i^ϕ), entropy (S_i^ϕ), and heat capacity (C_{Pi}^ϕ) data at 1 atm for all of the components (subscript i) of

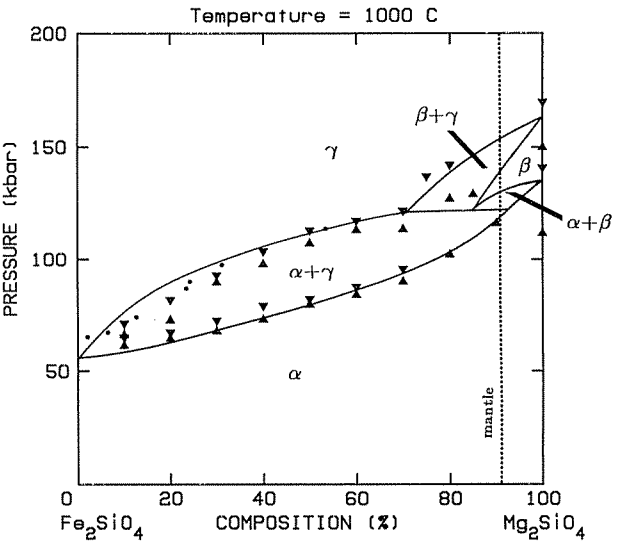

Fig. 2. Isothermal pressure-composition diagram [after *Jeanloz and Thompson*, 1983] showing experimental data for olivine polymorph stability fields at 1273 K. Data points [*Akimoto and Fujisawa*, 1968; *Ringwood and Major*, 1970; *Kawada*, 1977; *Suito*, 1977; *Yagi et al.*, 1979] denote the high-pressure stability limits of the low-pressure assemblages (triangles), the low-pressure stability limits of the high-pressure assemblages (inverse triangles), and the compositions of γ phase which coexist with α phase at the indicated pressures (dots).

interest in all of the phases (superscript ϕ) concerned. If high pressures are involved, a suitable equation of state, expressing the temperature and pressure dependence of the volume $V_i^{\phi}(P,T)$, is necessary, and if the phases are multicomponent, the relationships between the activities of the components (a_i^{ϕ}) and the compositions of the phases (X_i^{ϕ}) are also required.

Consider the free energy of Mg_2SiO_4 in the α phase. For pure α–Mg_2SiO_4 the free energy G^{α} at any pressure and temperature may be expressed as

$$G^{\alpha}_{Mg_2SiO_4}(P,T) = H^{\alpha}_{Mg_2SiO_4}(T_0) + \int_{T_0}^{T} C^{\alpha}_{P,Mg_2SiO_4}dT' - T\left(S^{\alpha}_{Mg_2SiO_4}(T_0) + \int_{T_0}^{T} \frac{C^{\alpha}_{P,Mg_2SiO_4}}{T'}\,dT'\right) + \int_{1}^{P} V^{\alpha}_{Mg_2SiO_4}(T)\,dP' \quad (1)$$

In equation (1), P and T refer to the pressure and temperature of interest, and enthalpy $H^{\alpha}_{Mg_2SiO_4}(T_0)$ and entropy $S^{\alpha}_{Mg_2SiO_4}(T_0)$ data are taken at 1 bar and some reference temperature T_0. The heat capacity (C_P) integrals take H and S from the reference temperature T_0 to the temperature of interest T at 1 bar, and the volume integral is performed at the temperature of interest T.

The conditions of equilibrium between pure Mg_2SiO_4 in the α phase and pure Mg_2SiO_4 in the β phase may be calculated by formulating a similar expression for β–Mg_2SiO_4 and equating the two free energy equations. For the equilibrium

$$\begin{array}{ccc} Mg_2SiO_4 & = & Mg_2SiO_4 \\ \alpha\text{–phase} & & \beta\text{–phase} \end{array} \quad (2)$$

we have at equilibrium with both phases pure

$$\Delta G = 0 = G^{\beta}_{Mg_2SiO_4}(P,T) - G^{\alpha}_{Mg_2SiO_4}(P,T) \quad (3)$$

Equations (1) and (3) may be solved for the univariant P-T curve which corresponds to equilibrium coexistence of α–Mg_2SiO_4 and β–Mg_2SiO_4. Natural olivines, however, contain at least one other component (Fe_2SiO_4) in addition to Mg_2SiO_4, so that the $\alpha+\beta$ equilibrium is divariant rather than univariant, as depicted in Figures 1 and 2. In solid solutions the free energy equations (1) and (2) have to be modified by taking account of the activities $a^{\alpha}_{Mg_2SiO_4}$ and $a^{\beta}_{Mg_2SiO_4}$ of the Mg_2SiO_4 component in the two phases of interest. The partial molar free energies $\overline{G}^{\alpha}_{Mg_2SiO_4}$ and $\overline{G}^{\beta}_{Mg_2SiO_4}$ are given [*Wood and Fraser*, 1977, pp. 52-53] by

$$\begin{aligned} \overline{G}^{\alpha}_{Mg_2SiO_4} &= G^{\alpha}_{Mg_2SiO_4} + RT \ln a^{\alpha}_{Mg_2SiO_4} \\ \overline{G}^{\beta}_{Mg_2SiO_4} &= G^{\beta}_{Mg_2SiO_4} + RT \ln a^{\beta}_{Mg_2SiO_4} \end{aligned} \quad (4)$$

and the condition of equilibrium (3) becomes

$$\Delta G = 0 = \overline{G}^{\beta}_{Mg_2SiO_4}(P,T) - \overline{G}^{\alpha}_{Mg_2SiO_4}(P,T) \quad (5)$$

With the standard state used here, the activity of Mg_2SiO_4 component in Mg_2SiO_4-Fe_2SiO_4 solid solution can take values between 0 (in pure Fe_2SiO_4) and 1 (in pure Mg_2SiO_4). In practice, Mg-Fe olivine solid solutions closely approximate ideal mixing behavior [*Navrotsky and Akaogi*, 1984]

$$a^{\alpha}_{Mg_2SiO_4}(P,T) \approx \left(X^{\alpha}_{Mg_2SiO_4}(P,T)\right)^2$$

where $X^{\alpha}_{Mg_2SiO_4}(P,T)$ is the mole fraction of Mg_2SiO_4 component in the α phase. Small positive deviations from ideality are observed for the α phase [*Wood and Kleppa*, 1981] so that an exact formulation for the activity is

$$a^{\alpha}_{Mg_2SiO_4}(P,T) = \left(X^{\alpha}_{Mg_2SiO_4}(P,T)\cdot\Gamma^{\alpha}_{Mg_2SiO_4}(P,T)\right)^2 \quad (6)$$

where the activity coefficient Γ is greater than 1 [*Wood and Kleppa*, 1981]. The appropriate substitutions in equations (4) and (5) show that at any P and T, the ratio of activities $a^{\beta}_{Mg_2SiO_4}(P,T)/a^{\alpha}_{Mg_2SiO_4}(P,T)$ is the parameter which can be found from the Mg_2SiO_4 equilibrium. This is insufficient to define the compositions of the two coexisting phases in the divariant region at any pressure and temperature. However, the presence of Fe_2SiO_4 component in both α and β phases yields the additional equilibrium condition

$$\begin{array}{ccc} Fe_2SiO_4 & = & Fe_2SiO_4 \\ \alpha\text{–phase} & & \beta\text{–phase} \end{array}$$

for which

$$\Delta G = 0 = \overline{G}^{\beta}_{Fe_2SiO_4}(P,T) - \overline{G}^{\alpha}_{Fe_2SiO_4}(P,T)$$

with $\overline{G}$ given by

$$\begin{aligned} \overline{G}^{\alpha}_{Fe_2SiO_4} &= G^{\alpha}_{Fe_2SiO_4} + RT \ln a^{\alpha}_{Fe_2SiO_4} \\ \overline{G}^{\beta}_{Fe_2SiO_4} &= G^{\beta}_{Fe_2SiO_4} + RT \ln a^{\beta}_{Fe_2SiO_4} \end{aligned} \quad (7)$$

Solving for the ratios of both sets of activities $a^{\beta}_{Mg_2SiO_4}(P,T)/a^{\alpha}_{Mg_2SiO_4}(P,T)$ and $a^{\beta}_{Fe_2SiO_4}(P,T)/a^{\alpha}_{Fe_2SiO_4}(P,T)$ enables the determination, through activity-composition relations, of the compositions of the coexisting α and β phases in the divariant region. In practice, the nonlinear equations were solved numerically by the method described in Appendix A.

Equations (1)-(7) above provide the basis of our method of solving for univariant and divariant equilibrium relations in the Mg_2SiO_4-Fe_2SiO_4 system. The thermodynamic data required by the equations are not all known, however, and those that are available are, in some cases, subject to considerable uncertainty. This has required certain approximations and assumptions which we shall outline here. First, heat capacities C_P are not known for the high-pressure polymorphs over the entire temperature range of interest. An extremely good simplification for solid-solid phase relations is that the heat capacity difference between high- and low-pressure phases is independent of temperature [*Wood and Holloway*, 1984], which is equivalent to fixing all of the heat capacities at the values for the reference temperature, in this case, 1000 K. Here we have used such constant 1000 K values (see Table 2 below), but we have performed parallel calculations using the estimated temperature dependencies of the heat capacities as given by *Watanabe* [1982] and found no departure from the behavior described herein. Second, it is necessary to assume an appropriate form for the equations of state of the α, β, and γ polymorphs of Mg_2SiO_4 and Fe_2SiO_4. We have used measured volume coefficients of thermal expansion, $\alpha(T)$, at 1 atm to obtain volumes at the temperature of interest T and 1 bar ($\sim$1 atm) pres-

sure. At constant pressure P the coefficient of thermal expansion is defined by

$$\alpha_i(T) \equiv \frac{1}{V_i(T)}\left(\frac{\partial V_i}{\partial T}\right)_P \tag{8}$$

(The coefficient of thermal expansion $\alpha(T)$, used as a thermodynamic parameter, should not be confused with the α phase of olivine, used as a superscript.) In the temperature range of interest, α is expected to increase linearly with T, attaining a limiting value at high temperatures [cf. *Ashcroft and Mermin*, 1976, pp. 490-495]. Representing this linear temperature dependence of α_i by

$$\alpha_i(T) = \alpha_i(298K) + \left(\frac{\partial \alpha_i}{\partial T}\right)_P (T - 298)$$

equation (8) may be integrated to give V at 1 bar and temperature T relative to the reference temperature of 298 K

$$V_i(T) = V_i(298)\ \exp\left[\alpha_i(298K)(T - 298) + \frac{1}{2}\left(\frac{\partial \alpha_i}{\partial T}\right)_P (T^2 - 298^2) - 298\left(\frac{\partial \alpha_i}{\partial T}\right)_P (T - 298)\right] \tag{9}$$

(We have a performed parallel analysis with α fixed at its linearly extrapolated 1200 K value (see Table 2 below) and found that our computed phase relations are not sensitive to this assumption.)

In order to integrate the VdP term in equation (1), the pressure dependence of V at temperature T is needed, requiring introduction of the isothermal bulk modulus K_T

$$K_T(T) \equiv -V(T)\left(\frac{\partial P}{\partial V}\right)_T \tag{10}$$

Most of the available bulk modulus data were obtained at 298 K rather than at high temperature, and they generally refer to adiabatic (K_S) rather than isothermal (K_T) values. To take account of these differences, we have used constant values of the Anderson-Grüneisen ratio δ_S as follows [cf. *Anderson et al.*, 1968]

$$\delta_S \equiv \frac{-1}{\alpha K_S}\left(\frac{\partial K_S}{\partial T}\right)_P \tag{11}$$

$$K_T = \frac{K_S}{1 + T\alpha\gamma} \tag{12}$$

$$\left(\frac{\partial K_T}{\partial P}\right)_T = \frac{\left(\frac{\partial K_S}{\partial P}\right)_T}{1 + T\alpha\gamma} \tag{13}$$

where the Grüneisen parameter γ is given by

$$\gamma \equiv \frac{\alpha K_S V}{C_P}$$

These relationships provide the pressure and temperature dependencies of the isothermal bulk modulus K_T. In accordance with the Eulerian finite strain formulation of *Birch* [1952], we have used the isothermal bulk modulus and its pressure derivative in conjunction with the third order Birch-Murnaghan isothermal state equation to obtain the implicit pressure dependence of the volume

$$P = \frac{3}{2}K_T(T)\left[\left(\frac{V(1,T)}{V(P,T)}\right)^{\frac{7}{3}} - \left(\frac{V(1,T)}{V(P,T)}\right)^{\frac{5}{3}}\right]\left\{1 - \frac{3}{4}\left[4 - \left(\frac{\partial K_T}{\partial P}\right)_T\right]\left[\left(\frac{V(1,T)}{V(P,T)}\right)^{\frac{2}{3}} - 1\right]\right\} \tag{14}$$

In equation (14), the isothermal bulk modulus K_T and its pressure derivative are evaluated at 1 bar and the temperature of interest, and V(1,T) and V(P,T) refer to the volume of the phase at 1 bar and temperature T and at P bars and temperature T, respectively. To evaluate G as a function of pressure, the VdP term in the free energy equation (1) was integrated using a composite rectangular quadrature scheme [cf. *Forsythe et al.*, 1977, pp. 85-89]; at each evaluation point of the quadrature, a one-dimensional Newton's method [cf. *Gerald and Wheatley*, 1984, pp. 15-20] was used to evaluate V as a function of P by equation (14) within 1-bar precision in pressure.

Interrelationship Between Thermodynamic and Experimental Data

The formalism discussed above enables the calculation of the partial molar free energies of Mg_2SiO_4 and Fe_2SiO_4 components in α, β, and γ phases at any desired pressure and temperature. Hence univariant boundaries and divariant fields may be calculated in pressure-temperature-composition space. While most of the necessary thermodynamic parameters have been measured within some experimental uncertainty, data for certain of the parameters simply do not exist. For example, thermodynamic data for the metastable β–Fe_2SiO_4 phase are unknown, although they are required for the calculation procedure (equation (7)). Furthermore, activity-composition data for the β and γ phases are unknown, and the pressure and temperature derivatives of the bulk moduli of β and γ phases are extremely uncertain. Fortunately, the measured phase relations in the Mg_2SiO_4-Fe_2SiO_4 system (Figure 2), although incomplete, may be used to constrain and refine unknown and uncertain thermodynamic properties. This can be done simply by inverting the formal calculation procedure discussed in the context of equations (1)-(7). The measured phase diagram has the requirement that when two phases coexist, $\Delta G = 0$ (equation (3)) for the equilibrium of interest, thus the thermodynamic properties must be consistent with equilibrium under the pressure-temperature-composition conditions which are measured. This is the major test of internal consistency of the thermodynamic data set.

Phase diagram measurements which have been used to construct an internally consistent model of the Mg_2SiO_4-Fe_2SiO_4 system are summarized in Table 1. In general, where several measurements of the same reaction have been made, those implying equilibrium at the lowest pressure have been adopted. This is because anvil devices used in high-pressure experiments tend, because of friction loss, to overestimate equilibrium pressure. Furthermore, when experiments start with the low-pressure α phase, as most do, reaction kinetics require a certain overstepping of the equilibrium pressure to higher pressure before the high-pressure phase begins to grow. Since both of these

TABLE 1. Phase Diagram Constraints on Thermodynamic Data Set

Measurement	Constrains (Primarily)	References for Data
P of α–$Mg_2SiO_4 \rightarrow \beta$–$Mg_2SiO_4$	$G^{\beta}_{Mg_2SiO_4} - G^{\alpha}_{Mg_2SiO_4}$	*Ringwood and Major* [1970], *Kawada* [1977], *Suito* [1977]
P of β–$Mg_2SiO_4 \rightarrow \gamma$–$Mg_2SiO_4$	$G^{\gamma}_{Mg_2SiO_4} - G^{\beta}_{Mg_2SiO_4}$	*Suito* [1977], *Yagi et al.* [1979], *Kawada* [1977]
P of α–$Fe_2SiO_4 \rightarrow \gamma$–$Fe_2SiO_4$	$G^{\gamma}_{Fe_2SiO_4} - G^{\alpha}_{Fe_2SiO_4}$	*Kawada* [1977], *Ringwood and Major* [1970], *Akimoto and Fujisawa* [1968]
$\alpha+\gamma$ divariant loop	nonideality of γ phase	*Akimoto and Fujisawa* [1968], *Ringwood and Major* [1970], *Kawada* [1977]
$\beta+\gamma$ divariant loop	nonideality of β phase	*Kawada* [1977], *Nishizawa and Akimoto* [1973], *Akaogi and Akimoto* [1979]
$\alpha+\gamma \rightarrow \beta$ reaction	$G^{\beta}_{Fe_2SiO_4} - G^{\alpha}_{Fe_2SiO_4}$	*Kawada* [1977], *Ringwood and Major* [1970]
P-T slope of α–$Mg_2SiO_4 \rightarrow \beta$–$Mg_2SiO_4$	$S^{\beta}_{Mg_2SiO_4} - S^{\alpha}_{Mg_2SiO_4}$	*Kawada* [1977], *Suito* [1977]
P-T slope of β–$Mg_2SiO_4 \rightarrow \gamma$–$Mg_2SiO_4$	$S^{\gamma}_{Mg_2SiO_4} - S^{\beta}_{Mg_2SiO_4}$	*Kawada* [1977], *Suito* [1977], *Sawamoto* [1985]
P-T slope of α–$Fe_2SiO_4 \rightarrow \gamma$–$Fe_2SiO_4$	$S^{\gamma}_{Fe_2SiO_4} - S^{\alpha}_{Fe_2SiO_4}$	*Akimoto et al.* [1977]

effects would lead to overestimation of equilibrium pressure, the lowest measured value for a particular reaction is generally to be preferred. (A. Navrotsky and M. Akaogi have recently pointed out to us that problems of thermal expansion and phase changes in the pressure medium, together with difficulties of high-temperature pressure calibration, can also lead to underestimation of equilibrium pressure. We have performed a preliminary analysis using data which yield slightly higher pressures of α–β Mg_2SiO_4 equilibrium (M. Akaogi, personal communication, 1986) than those adopted here. We find that while the absolute values of our derived enthalpies change, bringing them into better agreement with those reported by *Akaogi et al.* [1984] and *Navrotsky and Akaogi* [1984], the topology of our computed phase diagram, including the width of the $\alpha+\beta$ loop, does not change significantly.) Finally, it should be noted that while we assume that the results of the synthesis experiments are indicative of chemical equilibrium, very few of these experiments have rigorously demonstrated equilibrium according to the criterion of "reversibility" [*Fyfe*, 1960].

The transition pressure for α–$Fe_2SiO_4 \rightarrow \gamma$–$Fe_2SiO_4$ was taken from *Kawada* [1977] and *Akimoto et al.* [1977] and fixed at 60 kbar at 1000°C. The $\alpha \rightarrow \beta$ and $\beta \rightarrow \gamma$ transitions in Mg_2SiO_4 were taken, at 1000°C, to be 120 kbar [*Ringwood and Major*, 1970] and 160 kbar [*Yagi et al.*, 1979], respectively. The metastable transition of α–Fe_2SiO_4 to β–Fe_2SiO_4 was fixed to have a free energy change of +6000 cal/mol at 1 bar and 1000°C. This comes from the approximate position in pressure-composition space of the α–β–γ univariant line, as given by *Kawada* [1977] and by *Ringwood and Major* [1970], and gives a metastable $\alpha \rightarrow \beta$ transition pressure of 94 kbar, in excellent agreement with the estimated value of 92 kbar given by *Navrotsky and Akaogi* [1984].

The nonideal mixing properties of the α-phase were taken from *Wood and Kleppa* [1981] and *Fisher and Medaris* [1969] and may be represented by the two-site subregular solution model [cf. *Thompson*, 1967] as follows

$$a^{\alpha}_{Mg_2SiO_4} = \left(X^{\alpha}_{Mg_2SiO_4}\,\Gamma^{\alpha}_{Mg_2SiO_4}\right)^2$$

$$a^{\alpha}_{Fe_2SiO_4} = \left(X^{\alpha}_{Fe_2SiO_4}\,\Gamma^{\alpha}_{Fe_2SiO_4}\right)^2$$

where

$$\begin{aligned} RT \ln \Gamma^{\alpha}_{Mg_2SiO_4} &= \left(X^{\alpha}_{Fe_2SiO_4}\right)^2 \left[W^{\alpha}_{Mg_2SiO_4} + 2X^{\alpha}_{Mg_2SiO_4}\left(W^{\alpha}_{Fe_2SiO_4} - W^{\alpha}_{Mg_2SiO_4}\right) + PW^{\alpha}_{V}\right] \\ RT \ln \Gamma^{\alpha}_{Fe_2SiO_4} &= \left(X^{\alpha}_{Mg_2SiO_4}\right)^2 \left[W^{\alpha}_{Fe_2SiO_4} + 2X^{\alpha}_{Fe_2SiO_4}\left(W^{\alpha}_{Mg_2SiO_4} - W^{\alpha}_{Fe_2SiO_4}\right) + PW^{\alpha}_{V}\right] \end{aligned} \quad (15)$$

These activity-composition relations were used to derive the $W^{\gamma}_{Mg_2SiO_4}$ and $W^{\gamma}_{Fe_2SiO_4}$ Margules parameters (Table 2) from the $\alpha+\gamma$ divariant loop determined experimentally by *Ringwood and Major* [1970]. A similar approach for partitioning in the $\beta+\gamma$ divariant field [*Nishizawa and Akimoto*, 1973; *Akaogi and Akimoto*, 1979] gave the $W^{\beta}_{Mg_2SiO_4}$ and $W^{\beta}_{Fe_2SiO_4}$ terms of Table 2, with the available data being insufficiently precise to require any asymmetry in mixing properties. The results are consistent with the data of *Nishizawa and Akimoto* [1973], who concluded that both the α and γ phases exhibit positive deviations from ideality ($\Gamma > 1$ and $W > 0$) at high pressure. Since the W^{α} and W^{γ} terms have similar magnitudes but opposite asymmetries, our fitting procedure also supports the suggestion of *Navrotsky and Akaogi* [1984] that the nonidealities in these two phases largely cancel one another out when activity ratios for the $\alpha+\gamma$ field are calculated.

The logarithmic temperature derivatives of the bulk moduli, in the form of Anderson-Grüneisen ratios (equation (11)), are given by *Jeanloz and Thompson* [1983] for α–Mg_2SiO_4 and α–Fe_2SiO_4. To obtain estimates of the temperature dependence of the bulk moduli for the β and γ phases, we have made use of the empirical observation

TABLE 2. Internally Consistent Data Base Consistent With Experimental Data

	Component					
	Mg_2SiO_4	Fe_2SiO_4	Mg_2SiO_4	Fe_2SiO_4	Mg_2SiO_4	Fe_2SiO_4
Phase	α	α	β	β	γ	γ
S°_{1000K}, cal/K	66.23[a]	83.47[b]	64.21[c]	81.43[c]	63.68[c]	80.87[c]
Range: H°_{1000K}, cal	-14,970±270[d]	-6,560±310[e]	-7,980±730[f]	-2,652±780[g]	-6,350±930[f]	-5,857±840[g]
Value	-15140.	-6560.	-9595.	-3161.	-7112.	-3897.
C_P^{1000K}, cal/K	41.58[h]	46.18[h]	40.78[h]	46.06[i]	39.72[h]	45.90[h]
V(1,298), cm^3	43.67[j]	46.27[j]	40.52[j]	43.22[j]	39.65[j]	42.02[j]
α(298 K) $\times 10^6$, K^{-1}	26.08[j]	26.18[j]	20.63[j]	22.1[i]	18.63[j]	21.16[j]
$(\partial\alpha/\partial T)_P \times 10^6$, K^{-2}	0.015[j]	0.012[j]	0.017[j]	0.011[i]	0.017[j]	0.011[j]
α(1200 K) $\times 10^6$, K^{-1}	39.97[k]	37.00[k]	35.72[k]	32.0[k]	33.72[k]	31.56[k]
Range: K_{0S}, Mbar	1.28-1.30[l]	1.36-1.39[l]	1.68-1.80[m]	1.83-1.95[l]	1.81-1.87[l]	1.96-2.02[l]
Value	1.29	1.38	1.74	1.89	1.84	1.99
Range: $(\partial K_S/\partial P)_T^{(1,300K)}$	5.0-5.4[j]	5.0-5.4[j]	3.0-5.0[j]	3.0-5.0[j]	3.8-5.8[j]	3.8-5.8[j]
Value	5.2	5.2	4.8	4.8	4.8	4.8
γ_{1000K}	1.20[k]	1.10[k]	1.3[k]	1.3[k]	1.35[k]	1.25[k]
δ_S	4.0[j]	5.5[j]	4.3[c]	5.6[c]	4.3[c]	5.8[c]
W, cal	2000.[n]	1000.[n]	1500.[c]	1500.[c]	1000.[c]	2000.[c]
W_V, cal/bar	0.003[o]	0.003[o]	0.	0.	0.	0.
Range: μ_0, Mbar	0.80-0.82[l]	0.50-0.52[l]	1.08-1.20[m]	0.67-0.79[l]	1.16-1.22[l]	0.75-0.81[l]
Value	0.81	0.51	1.14	0.73	1.19	0.78
$(\partial\mu/\partial P)_T$	1.82[p]	0.62[p]	1.8[c]	0.6[c]	1.8[c]	0.6[c]
$(-1/\mu)(\partial\mu/\partial T)_P$, K^{-1}	0.00017[p]	0.00021[p]	0.0002[c]	0.0002[c]	0.0002[c]	0.0002[c]

Phases are olivine (α), modified spinel (β), and spinel (γ). S°_{1000K} is third law entropy at 1000 K, H°_{1000K} enthalpy of formation from oxides at 1000 K and 1 bar, C_P^{1000K} isobaric heat capacity at 1000 K, V(1,298) volume at 1 bar and 298 K, α(298 K) thermal expansion at 298 K and 1 bar, α(1200 K) thermal expansion in the high-temperature limit at 1 bar, K_{0S} adiabatic bulk modulus at 300 K and 1 bar, μ_0 zero-pressure shear modulus at 300 K and 1 bar, γ_{1000K} Grüneisen ratio computed at 1000 K, δ_S Anderson-Grüneisen parameter. W and W_V are the excess internal energies and volumes, respectively, of solution given on a per site basis. (For example, W for α–Mg_2SiO_4 is the 1-bar excess enthalpy of putting an Mg atom into a site occupied by an Fe atom in the α phase.) Observed ranges and best fit values are given for bulk moduli, their pressure derivatives, shear moduli, and enthalpies.

[a] *Robie et al.* [1978].
[b] *Robie* [1982].
[c] Estimated as discussed in text.
[d] *Wood and Holloway* [1984].
[e] *Wood and Holloway* [1982].
[f] *Akaogi et al.* [1984].
[g] Estimated by *Navrotsky and Akaogi* [1984].
[h] *Watanabe* [1982].
[i] Estimated from values for α and γ phases and β–Mg_2SiO_4.
[j] *Jeanloz and Thompson* [1983].
[k] Computed from data given above.
[l] *Weidner et al.* [1984].
[m] *Sawamoto et al.* [1984].
[n] *Wood and Kleppa* [1981].
[o] *Fisher and Medaris* [1969].
[p] *Sumino and Anderson* [1984].

[*Anderson et al.*, 1968] that the logarithmic temperature derivatives of the bulk moduli of most mantle minerals are approximately the same, of order 10^{-4} K^{-1}. We have assumed, then, that the logarithmic temperature derivative of the bulk modulus for a given component (Mg_2SiO_4 or Fe_2SiO_4) in the β or γ phase is approximately the same as that of the same component in the α phase, giving the consequent Anderson-Grüneisen ratios (δ_S's) shown in Table 2. Uncertainties in this parameter have much smaller effects on our computed phase relationships than do the experimental uncertainties in bulk moduli discussed below.

RESULTS

The combination of experimental and thermodynamic data discussed above enabled us to calculate the internally consistent phase diagram shown in Figure 3. As can be seen, the $\alpha+\beta$ divariant field is extremely narrow at 1000°C, giving a loop which is only about 2 kbar wide. Furthermore, at this temperature, olivine with a presumed mantle Mg/(Mg+Fe) ratio (~0.9) undergoes a transition from the α to the β phase with increasing pressure which, although strictly divariant ($\alpha \rightarrow \alpha+\beta \rightarrow \beta$) in nature, is effectively univariant ($\alpha \rightarrow \beta$) with respect to width and so

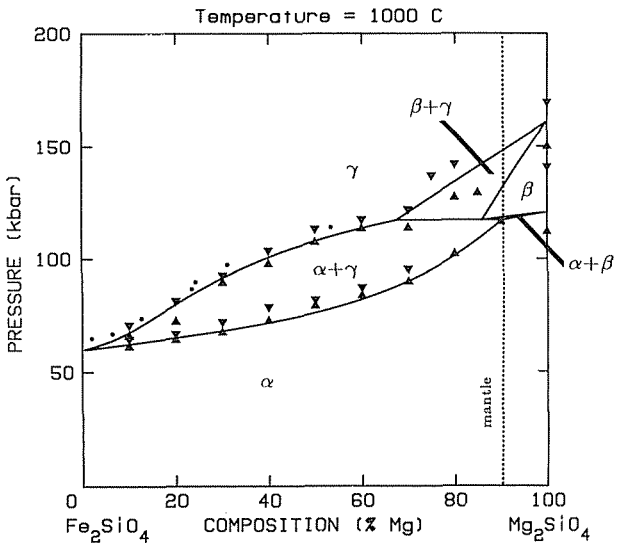

Fig. 3. Internally consistent isothermal pressure-composition diagram showing calculated boundaries (from Table 2) for olivine polymorph stability fields at 1273 K. Also shown are experimental data from Figure 2.

would give rise to a sharp change in elastic properties and seismic velocities over a narrow depth interval (~6 km).

Using measured values of the pressure-temperature slopes of the $\alpha \rightarrow \beta$ and $\beta \rightarrow \gamma$ transitions in Mg_2SiO_4 [*Kawada*, 1977; *Suito*, 1977; *Sawamoto*, 1986] and the $\alpha \rightarrow \gamma$ transition in Fe_2SiO_4 [*Akimoto et al.*, 1977], we extracted (equation (1)) values of ΔS°, and hence ΔH°, from the ΔG°, ΔV°, and C_P data discussed above. The values of ΔH° thus obtained (Table 2) are slightly smaller in magnitude, in general, than those given by *Akaogi et al.* [1984] and *Navrotsky and Akaogi* [1984] but still close to their experimental measurements. Together with reference values for the standard state entropies [*Robie et al.*,, 1978; *Robie*, 1982] and enthalpies [*Wood and Holloway*, 1982, 1984] of the α-olivine components, these values of ΔH° and ΔS° complete the set of data necessary for calculation of a pressure-composition diagram (Figure 4) at 1500°C, a reasonable temperature for the pressures corresponding to 400 km depth in the earth [*Bott*, 1982, pp. 170-175]. As can be seen, increasing temperature narrows the $\alpha+\beta$ divariant loop (to about 1 kbar width), and the $\alpha \rightarrow \beta$ transition in mantle olivine would take place at about 135 kbar, corresponding to 405 km depth in the earth. Our analysis, unlike the simpler approach of *Navrotsky and Akaogi* [1984], does not produce transformation of mantle olivine to $\alpha+\gamma$ phases before the stability field of the β phase is reached (Figures 3 and 4). We therefore conclude that a sharp seismic discontinuity over a very narrow depth interval would attend the transformation of $(Mg_{0.9}Fe_{0.1})_2SiO_4$ olivine to the β phase at about 400-km depth.

Sensitivity Analysis

We have investigated the robustness of our conclusion that the $\alpha \rightarrow \beta$ phase transformation in olivine should produce a seismic signature appropriate for a sharp 400-km discontinuity, relative to uncertainties in the experimental and thermodynamic data. The important results of our sensitivity analysis of the dependence of the calculated phase relations on errors in the data are summarized in Table 3. Most of the features of the phase diagrams of Figures 3 and 4 are extremely robust relative to perturbations of the constraining parameters, a significant exception being the relationship between β and γ phases at high temperatures.

Uncertainties in β–γ phase relations arise primarily from uncertainties in the P-T slope of the $\beta \rightarrow \gamma$ phase transition in Mg_2SiO_4. Because of the small volume change of the $\beta \rightarrow \gamma$ reaction at low pressure (Table 2) and the poorly known pressure derivatives of the bulk moduli, small uncertainties in the entropy change of reaction lead to large uncertainties in the computed pressure-temperature slopes. Although *Kawada* [1977] determined the pressure-temperature slope of the $\beta \rightarrow \gamma$ transition, his data may have appreciable uncertainties in pressure calibration at pressures above 120 kbar [*Sawamoto*, 1986]. The data of *Suito* [1977] and *Sawamoto* [1986], however, constrain the $\beta \rightarrow \gamma$ transition in Mg_2SiO_4 to fall within a ±10 kbar range (i.e., 535-595 km depth) at 1500°C (Table 3).

In contrast to the $\beta+\gamma$ loop, the $\alpha+\beta$ loop, which is considered to produce the 400-km seismic discontinuity, is extremely well constrained by the experimental and thermodynamic data. Decreases in the standard state free energy of metastable β-Fe_2SiO_4 can widen the loop slightly, to almost 3 kbar, but beyond this point, β-Fe_2SiO_4 would become stable in between the α and γ phases, a condition which is never observed experimentally. A 3-kbar (~9 km) width of the loop is therefore the maximum consistent with β-Fe_2SiO_4 being unstable. Perturbation of bulk moduli, heat capacities, thermal expansions, and activity relations all have extremely small effects on the width and position of the divariant field. It is effectively constrained by the moderate ΔV of reaction, the form of the $\alpha+\gamma$ loop in iron-rich compositions, and the positions of the $\alpha \rightarrow \beta$ and $\beta \rightarrow \gamma$ transitions in Mg_2SiO_4. Variation of the latter through the observed ranges does not open up the divariant $\alpha+\beta$ loop to any substantial extent.

Application to the 400-km Seismic Discontinuity

Having obtained a complete set of thermodynamic data for the α, β, and γ phases (Table 2), we calculated the

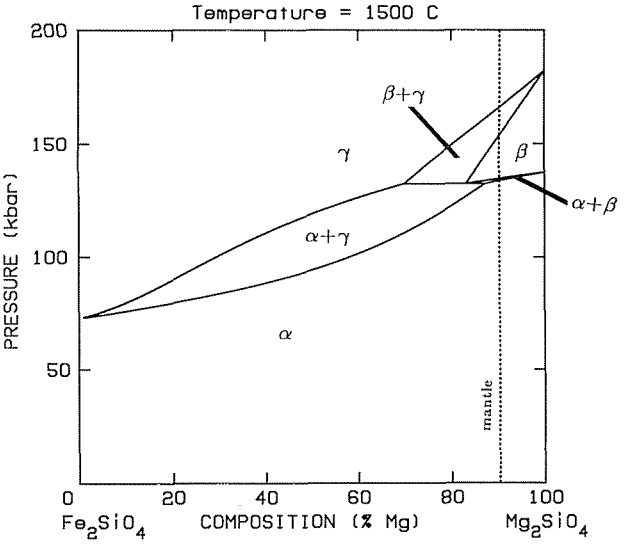

Fig. 4. Internally consistent isothermal pressure-composition diagram showing computed boundaries (from Table 2) for olivine polymorph stability fields at 1773 K.

TABLE 3. Sensitivity Analysis

Phase Diagram Feature	Variable	Sensitivity
Width of the $\alpha+\beta$ divariant phase loop	C_P	negligible
	α	negligible
	$G^{\beta}_{Fe_2SiO_4} - G^{\alpha}_{Fe_2SiO_4}$	<1 kbar to ~ 3 kbar
	activity relations	small ($\pm<1$ kbar)
	volume and bulk modulus	negligible
Width and position of the $\beta+\gamma$ divariant phase loop	C_P	negligible
	α	negligible
	volume and bulk modulus	up to ± 5 kbar uncertainty
	entropy	up to ± 10 kbar uncertainty

stable phase assemblages and mineral compositions as functions of temperature and pressure for pure olivine of composition $(Mg_{0.9}Fe_{0.1})_2SiO_4$. Such an olivine constitutes the major component of model peridotitic mantles [*Ringwood*, 1975; *Weidner*, 1985]. If the 400-km seismic discontinuity reflects an isochemical phase transition of α-olivine to β-modified-spinel, then the magnitude of the observed discontinuity should be comparable to that calculated, and observed and calculated seismic velocities should be similar. In practice, phase relations along isotherms at 1700 K and 2000 K were calculated from the thermodynamic data by a modification of the method of free energy minimization described by *Storey and Van Zeggeren* [1964] (see Appendix B). From the volume and thermoelastic data of Table 2, the density (ρ), volume-averaged bulk modulus, and bulk sound velocity ($\sqrt{\Phi}$) were calculated for each stable phase assemblage from the equation

$$\Phi = \frac{K_S}{\rho}$$

(In computing the volume-weighted averages of the adiabatic elastic moduli, we have used the Voigt-Reuss-Hill averaging technique. *Watt et al.* [1976] showed that for the case of coexisting forsterite and spinel, this average falls within the tightly constrained Hashin-Shtrikman bounds.)

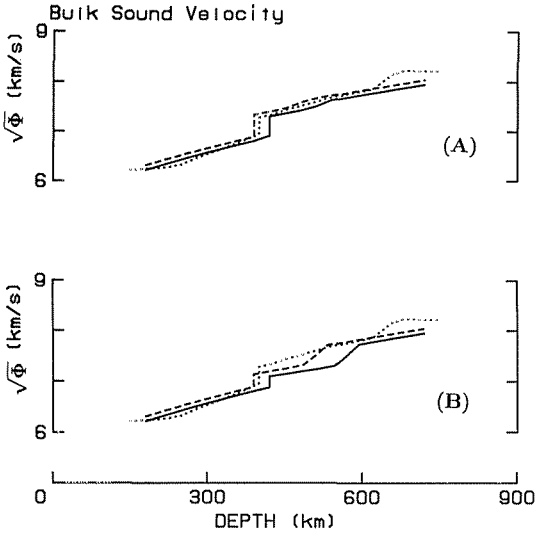

Fig. 5. (*a*) Calculated bulk sound velocity ($\sqrt{\Phi}$) as a function of depth for a mantle consisting of pure olivine of $(Mg_{0.9}Fe_{0.1})_2SiO_4$ composition, along 1700 K (dashed) and 2000 K (solid) isotherms for $\Delta K'_{\beta\gamma}$ of zero. (*b*) Same as 5(a) but for $\Delta K'_{\beta\gamma}$ of 0.8. Composite seismic profile GCA+TNA (dotted) is shown for comparison (see text for references).

Figure 5 shows calculated bulk sound velocity profiles through the 200- to 670-km depth interval for the pure olivine mantle composition. A sharp discontinuity in bulk sound velocity occurs at about 135 kbar (405 km) due to the $\alpha \rightarrow \beta$ transition. The magnitude of the velocity increase associated with the discontinuity is calculated to be about 6.6%. Our model exhibits no discontinuity or change in slope due to the $\beta \rightarrow \gamma$ transition because the volumes and elastic moduli of the β and γ phases are virtually identical in the depth interval 535-595 km in which that transition occurs. (It should be noted that in this study, we have not incorporated the effects of any higher pressure phases, such as silicate perovskite, which might contribute to the 650-km seismic discontinuity.)

Uncertainties in the pressure derivatives (K') of the bulk moduli of the β and γ phases can alter the calculated seismic velocities without violating the thermodynamic and phase equilibrium constraints that we have used. Because of their structural similarities and virtually identical bulk moduli at 1 atm [*Weidner et al.*, 1984; *Sawamoto et al.*, 1984], it is reasonable to assume that the pressure derivatives K'_β and K'_γ are the same. This assumption, which is consistent with the phase diagram, is that which was made to construct Figure 5*a*. Based on the quoted ranges of K' estimates, however [*Jeanloz and Thompson*, 1983], a difference between β and γ phases ($K'_\gamma - K'_\beta$) of up to 0.8 is plausible. If we were to adopt such a difference, the $\beta \rightarrow \gamma$ transition would become evident in bulk sound velocity profiles (Figure 5*b*), giving rise to an associated velocity increase near 550 km and so decreasing the magnitude of the discontinuous velocity increase associated with the $\alpha \rightarrow \beta$ transition at 400 km. Adopting $K'_\gamma - K'_\beta$ of 0.8 leaves a velocity increase of about 3.3% at 405 km and introduces a (less sharp) velocity increase of about 5.7% at about 550 km.

In order to use our computed bulk sound velocity profiles to draw conclusions about the composition of the mantle, we require observed seismic profiles against which to compare them. Recent regional seismic studies have produced velocity profiles for either *P* wave velocities alone (e.g., T7 of *Burdick and Helmberger* [1978] for western North America, K8 of *Given and Helmberger* [1980] for northwestern Eurasia, GCA ("Gulf of California") and GCA′ of *Walck* [1984] for the Gulf of California spreading center and its environs, CAPRI of *Leven* [1985] for north central Australia) or for *S* wave velocities alone (e.g., TNA ("Tectonic North America") of *Grand and Helmberger* [1984] for tectonically active western North America, SNA ("Shield North America") of *Grand and Helmberger* [1984] for the Canadian shield) as shown in

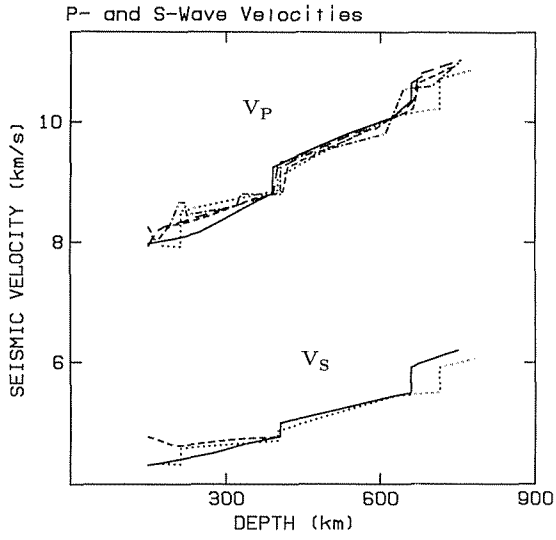

Fig. 6. Observed P and S wave velocities (V_P and V_S, respectively) as functions of depth from seismic studies, with PREM for comparison. P wave profiles are GCA (solid), T7 (long-dashed), K8 (short-dashed), CAPRI (dot-dashed), and PREM (dotted); S wave profiles are TNA (solid), SNA (dashed), and PREM (dotted) (see text for references).

Figure 6. However, as the square of the bulk sound velocity (Φ) represents a linear combination of the squares of the P and S wave velocities (equation (16) below), we require complementary observed P and S wave velocity profiles if we are to compare computed and observed values of $\sqrt{\Phi}$. The Φ profile given in the globally averaged seismic model PREM ("preliminary reference earth model") of *Dziewonski and Anderson* [1981] is not appropriate for such comparisons because the increases in P and S wave velocities at 400 km in PREM (2.6% and 3.4%, respectively) are in very poor agreement (Figure 6) with those observed in the detailed regional studies mentioned above (4.5-6.0%, and 4.6%, respectively). In order to compare $\sqrt{\Phi}$ profiles we have constructed a composite seismic profile ("GCA+TNA") for the tectonically active portion of western North America by combining the P wave data from *Walck*'s [1984] GCA study with the S wave data from the TNA study of *Grand and Helmberger* [1984]. The applicability of our results, however, is not limited to this region since, as shown in Figure 6, both the character of the 400-km discontinuity and the magnitudes of the seismic velocities from 300 to 600 km depth are quite robust throughout the various observed seismic profiles (with the notable exception of PREM). The slight variability in the depth (395-410 km) to the "400-km" discontinuity in these models may be ascribed to differences in assumed shallow structure [*Walck*, 1984].

The composite model GCA+TNA possesses an increase in bulk sound velocity of 4.9% at 400-km depth. Since our model pure olivine mantle (Figure 5*a*) produces a 6.6% increase at this depth, a mantle consisting of approximately 74% olivine would be consistent with the composite seismic observations. For the case shown in Figure 5*b*, where the difference in K' values of 0.8 displaces a portion of the velocity jump at 400 km to a depth of about 550 km, the 400-km velocity increase of 3.3% would be consistent with a mantle composed of 100% olivine. In making these mantle compositional estimates from the relative magnitudes of velocity increases, we have assumed that the nonolivine components of the mantle do not produce significant velocity variations over the ~6 km depth interval of interest. Inclusion of velocity variations due to nonolivine components (e.g., adopting eclogitic velocities from *Bina and Wood* [1984] for the remaining mantle constituents) alters these compositional estimates by a maximum of about 5%.

The most conservative assumption, leading to the minimum estimated amount of olivine in the mantle, is that $K'_\gamma - K'_\beta$ is 0.0. As shown above, the magnitude of the 400-km bulk sound velocity increase in GCA+TNA implies about 74% olivine in the mantle if this assumption is made. Calculated bulk sound velocities for a pure olivine mantle are in excellent agreement (within ± 0.06 km/s) with those of GCA+TNA. It appears therefore that the mantle is peridotitic at the 400-km discontinuity with about 70% olivine (i.e., very similar to "pyrolite" [*Ringwood*, 1975]). This conclusion, which is in good agreement with that of *Weidner* [1985], contradicts the assertion [*Bass and Anderson*, 1984; *Anderson and Bass*, 1984, 1986] that olivine-rich mantle does not occur in the transition zone.

Although bulk sound velocities for an olivine-rich mantle agree well with GCA+TNA (Figure 5*a*), a stricter test of a mantle model would be the direct calculation of P and S wave velocities (V_P and V_S, respectively) as functions of depth. If the shear modulus μ is known at high pressure and temperature, then the bulk modulus and bulk sound velocity can be decomposed into V_P and V_S from the standard relationships

$$\Phi = \frac{K_S}{\rho} = \left(V_P\right)^2 - \frac{4}{3}\left(V_S\right)^2$$
$$\left(V_S\right)^2 = \frac{\mu}{\rho} \qquad (16)$$

The pressure and temperature derivatives of the shear modulus of the α phase are known only at low pressures [*Sumino and Anderson*, 1984], and those of the β and γ phases must be estimated from other minerals or by making some reasonable assumptions. In any case it is clear that calculated V_P and V_S values are much more uncertain than $\sqrt{\Phi}$. Comparisons of observed and calculated $\sqrt{\Phi}$ values, as given above, provide much better constraints upon mantle mineralogy than V_P and V_S comparisons. In the absence of measured pressure and temperature derivatives of shear moduli for the high-pressure olivine polymorphs, we have used two different approaches to resolve our model $\sqrt{\Phi}$ profiles into P and S wave velocity profiles. First, we have made use of the empirical observation [*Anderson et al.*, 1968] that the logarithmic temperature derivatives of the bulk moduli of most mantle minerals are approximately the same, of order 10^{-4} K^{-1}, we have assumed a similar relationship for the shear moduli, namely, that the logarithmic temperature derivative of the shear modulus [cf. *Sumino et al.*, 1977] for a given component (Mg_2SiO_4 or Fe_2SiO_4) in the β or γ phase (Table 2) is the same as that of the same component in the α phase. In the absence of experimental data the assumption that all the elastic moduli show similar temperature behavior appears to be the most reasonable. In order to obtain the pressure derivatives of the shear moduli, we made use of the result [*Anderson and Liebermann*, 1970] that minerals with identical coordination numbers and similar ratios of shear modulus to bulk modulus have very similar shear modulus pressure derivatives. We therefore assumed that

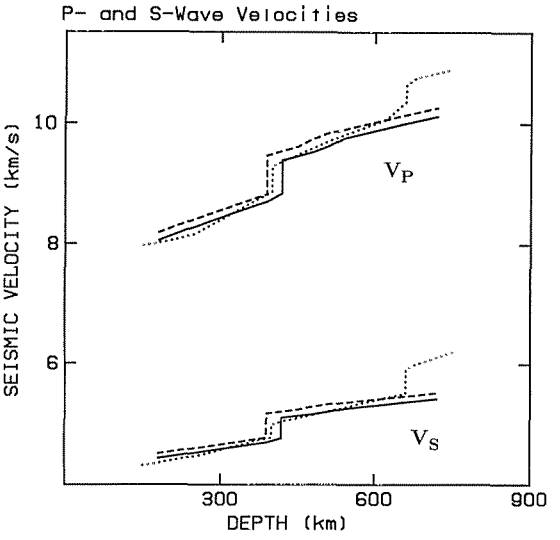

Fig. 7. Calculated P and S wave velocities (V_P and V_S, respectively) as functions of depth for a mantle consisting of pure olivine of $(Mg_{0.9}Fe_{0.1})_2SiO_4$ composition, along 1700 K (dashed) and 2000 K (solid) isotherms. Composite seismic profile GCA+TNA (dotted) is shown for comparison (see text for references).

the pressure derivative of the shear modulus for a given component in the β or γ phase (Table 2) is the same as that of the component in the α phase. Second, we have attempted to obtain V_P and V_S from Φ by the method employed by *Lees et al.* [1983]. Having computed the (Voigt-Reuss-Hill) average bulk modulus for the stable assemblage at a given pressure and temperature, we then assumed that Poisson's ratio for our model mantle at a given depth was identical to the value of Poisson's ratio at the corresponding depth in the GCA+TNA composite seismic profile. We then extracted the shear modulus μ from the aggregate bulk modulus K_S and Poisson's ratio σ according to the equation

$$\mu = \frac{3}{2}K_S\left(\frac{1-2\sigma}{1+\sigma}\right)$$

where σ is defined by

$$\sigma \equiv \frac{\frac{1}{2}\left(V_P/V_S\right)^2 - 1}{\left(V_P/V_S\right)^2 - 1}$$

and Poisson's ratio for this seismic velocity profile ranges from 0.286 to 0.297 in the region of interest. Although this second approach is somewhat circular, using observed values of Poisson's ratio to deduce the calculated model, we have included it here to facilitate comparison with the results of *Lees et al.* [1983].

The two "Φ decomposition" approaches yield almost identical velocity profiles. Figure 7 shows the results of calculated P and S wave velocities for pure $(Mg_{0.9}Fe_{0.1})_2SiO_4$ olivine as a function of depth for the first of these approaches, together with the composite seismic velocity profile GCA+TNA for comparison. As can be seen, there is close agreement between seismic velocities observed in the 200- to 650-km depth interval and those calculated by the methods outlined above for pure olivine. Based on the magnitude of the discontinuity at 400 km depth (4.8% and 4.5% increases in P and S wave velocity, respectively, for GCA+TNA; 7.2% and 8.1% for our model profiles), a mantle with approximately 62% olivine would be consistent with the seismic data. Thus, from the magnitudes of the increases in bulk sound velocity and in P and S wave velocities, we conclude that a mantle containing 62-74% olivine would be consistent with the seismic velocity data. This conclusion is in agreement with that of *Weidner* [1985] but is in conflict with the results of *Lees et al.* [1983] and with those of *Anderson and Bass* [1984, 1986] and *Bass and Anderson* [1984].

Lees et al. [1983] found that while the density profile of a pure olivine mantle would be quite consistent with that determined seismically, the P and S wave velocities for such a mantle would not be consistent with the seismic observations in the transition region. Their results, however, were based on elastic property estimates for the β and γ phases which are substantially in error [*Weidner et al.*, 1984]. *Lees et al.* [1983] remark that it would be necessary to lower the value of the bulk modulus of the γ phase in order to bring the computed and observed seismic velocities into agreement, and indeed, lowering the bulk modulus of the γ phase to the values measured by *Weidner et al.* [1984] and adopted by us (Table 2) brings a pure olivine mantle into much better agreement with the observed P and S wave velocities (Figure 7).

While the density [*Bass and Anderson*, 1984] and Φ [*Anderson and Bass*, 1984] profiles for an olivine-rich mantle composition ("pyrolite") are in agreement with current seismic observations, *Bass and Anderson* [1984] and *Anderson and Bass* [1986] found that the P and S wave velocities for an olivine-rich mantle were significantly higher that those for PREM. Examination of their elasticity data base (D. L. Anderson, personal communication, 1985) indicates that the values of the temperature derivatives of the shear moduli which they assumed for the β and γ phases imply a constant temperature derivative, rather than a constant logarithmic temperature derivative such as we have used here. The latter appears to be the better first approximation because it corresponds to observed bulk modulus behavior. Anderson and Bass's linear temperature extrapolation and reliance on spinel analog data result in larger shear moduli (and hence higher P and S wave velocities) at mantle temperatures and pressures. *Anderson and Bass* [1984] note that the seismic velocity data cannot rule out an olivine-rich upper mantle; however, we suggest that an olivine-rich mantle is not only consistent with the seismic velocities throughout the 200- to 650-km depth interval but is necessary to explain the sharpness and magnitude of the 400-km seismic discontinuity, short of invoking a discontinuity in bulk chemical composition at 400 km.

The actual sharpness of the 400-km discontinuity is difficult to resolve seismically [*Muirhead*, 1985]. *Kennett* [1975] discussed the possibility that mantle discontinuities may actually be much sharper than estimated by those seismic studies which neglect the effects of attenuation, and *Ingate et al.* [1986] have summarized the difficulties and uncertainties inherent in attempting to constrain gradients and discontinuities in seismic velocity by the technique of synthetic seismogram forward modeling. *Leven* [1985] suggests that the 400-km discontinuity occurs over a depth interval of about 6 km. Other studies [cf. *Silver et al.*, 1985] suggest that this discontinuity is at least 10 km wide. The $\alpha \rightarrow \beta$ transition width of approximately 6 km given herein is computed for isothermal conditions

and is actually sharper than required by most seismic data. The presence of temperature gradients through the transition [cf. *Verhoogen*, 1965; *Jeanloz and Thompson*, 1983] could broaden the discontinuity by a maximum of about 7 km.

CONCLUSIONS

In conclusion, by using available calorimetric, thermoelastic, and synthesis data we have derived an internally consistent high-pressure phase diagram for the Mg_2SiO_4-Fe_2SiO_4 join which is quite insensitive to the uncertainties in the experimental data. This diagram, in turn, constrains the divariant $\alpha \rightarrow \alpha+\beta \rightarrow \beta$ transition to be extremely sharp, effectively univariant on the scale of the mantle. For mantle olivine compositions, then, the $\alpha \rightarrow \alpha+\beta \rightarrow \beta$ transition in $(Mg_{0.9}Fe_{0.1})_2SiO_4$ should occur over a depth range (isothermal) of approximately 6 ($\pm$3) km at a depth of about 400 km. (The presence of temperature gradients through the transition may broaden the depth interval by a maximum of about 7 km.) This transition would produce a sharp discontinuity in seismic velocity at this depth, in excellent agreement with seismic observations.

The bulk sound velocity profile for a model mantle consisting of pure olivine is in good agreement with the observed seismic profiles, both above and below the 400-km discontinuity, so that an olivine-rich mantle is quite consistent with available seismic data. Furthermore, comparison of the observed magnitude of the velocity jump at 400-km depth with that computed for a pure olivine mantle suggests a mantle composed of about 70% olivine. Attempts at resolving individual P and S wave velocities from the elastic data produce computed seismic velocity profiles which are in good agreement with recent regional seismic models. The relative sizes of the computed and observed jumps in P and S wave velocities and bulk sound velocity across the discontinuity are indicative of a mantle containing 62-74% olivine. A mantle of olivine-rich composition is thus quite consistent with the current mineralogical and seismic data; the data do not require the transition zone to be chemically distinct from the uppermost mantle.

APPENDIX A: CALCULATION OF DIVARIANT PHASE RELATIONS

The system of equilibrium conditions in the divariant region $\alpha+\beta$ consists of equations (cf. equation (3)) of the form

$$\overline{G}^{\alpha}_{Mg_2SiO_4} = \overline{G}^{\beta}_{Mg_2SiO_4}$$

$$\overline{G}^{\alpha}_{Fe_2SiO_4} = \overline{G}^{\beta}_{Fe_2SiO_4}$$

We may define difference functions F such that

$$F_i^{\alpha\beta} \equiv \overline{G}_i^{\alpha} - \overline{G}_i^{\beta}$$

for each component i, and we may then seek solutions to equations of the form

$$F_i^{\alpha\beta}\left(X_1^{\alpha}, X_1^{\beta}, P, T\right) = 0$$

In the divariant region the requisite system of equations is simply

$$F_1^{\alpha\beta}\left(X_1^{\alpha}, X_1^{\beta}, P, T\right) = 0$$

$$F_2^{\alpha\beta}\left(X_1^{\alpha}, X_1^{\beta}, P, T\right) = 0$$

where $X_2^{\phi} = 1 - X_1^{\phi}$ for any given phase ϕ.

To solve for the case of equilibrium involving all three phases α, β, and γ, we need only include two more equations, those involving either the α-γ or the β-γ difference functions, in this system.

In order to solve the system, we may employ Newton's method [cf. *Gerald and Wheatley*, 1984, pp. 133-139] to reduce the solution of the system of nonlinear equations to iterations of solutions of systems of linear equations. We accomplish this by developing the first-order (i.e., linear) Taylor series approximation [cf. *Hurley*, 1980, pp. 710-714] to each function F_i, so that

$$\begin{aligned} 0 \approx &\left(F_1^{\alpha\beta}\right) + \left(\frac{\partial F_1^{\alpha\beta}}{\partial X_1^{\alpha}}\right)\left(X^{\alpha}_{1,new} - X^{\alpha}_{1,old}\right) \\ &+ \left(\frac{\partial F_1^{\alpha\beta}}{\partial X_1^{\beta}}\right)\left(X^{\beta}_{1,new} - X^{\beta}_{1,old}\right) \\ 0 \approx &\left(F_2^{\alpha\beta}\right) + \left(\frac{\partial F_2^{\alpha\beta}}{\partial X_1^{\alpha}}\right)\left(X^{\alpha}_{1,new} - X^{\alpha}_{1,old}\right) \\ &+ \left(\frac{\partial F_2^{\alpha\beta}}{\partial X_1^{\beta}}\right)\left(X^{\beta}_{1,new} - X^{\beta}_{1,old}\right) \end{aligned} \tag{A1}$$

where each function F_i and its derivatives are evaluated at the appropriate approximate root $X^{\phi}_{1,old}$.

We may use forward finite differences [cf. *Gerald and Wheatley*, 1984, pp. 233-238] for the calculation of derivatives, so that

$$\left(\frac{\partial F_1^{\alpha\beta}}{\partial X_1^{\alpha}}\right)_{P,T,X^{\beta}_{1,old}} \approx \frac{1}{\delta}\left[F_1^{\alpha\beta}\left(X^{\alpha}_{1,old}+\delta, X^{\beta}_{1,old}, P, T\right) - F_1^{\alpha\beta}\left(X^{\alpha}_{1,old}, X^{\beta}_{1,old}, P, T\right)\right]$$

$$\left(\frac{\partial F_1^{\alpha\beta}}{\partial X_1^{\beta}}\right)_{P,T,X^{\alpha}_{1,old}} \approx \frac{1}{\delta}\left[F_1^{\alpha\beta}\left(X^{\alpha}_{1,old}, X^{\beta}_{1,old}+\delta, P, T\right) - F_1^{\alpha\beta}\left(X^{\alpha}_{1,old}, X^{\beta}_{1,old}, P, T\right)\right]$$

where δ is some small finite perturbation parameter.

The linear systems (A1) may be solved by a matrix method, such as Gaussian elimination employing partial pivoting [cf. *Gerald and Wheatley*, 1984, pp. 88-95]. Each solution of a system such as (A1) will give the correction factors $(X^{\phi}_{1,new} - X^{\phi}_{1,old})$ by which the previous approximate solution $X^{\phi}_{1,old}$ must be modified, and hence values for $X^{\phi}_{1,new}$ may be obtained for all pertinent phases ϕ. These corrections may be applied iteratively until the absolute differences between consecutive solutions fall below some arbitrary tolerance value ϵ. Note that when solving the univariant problem for three coexisting phases numerically, it may be necessary to scale the pressure variable to the same order of magnitude as the composition (mole fraction) variables (i.e., order 10^{-1}) in order to avoid forming a nearly singular matrix during linearization.

Initial estimates of the solution variables for Newton's method may be obtained as follows. The partial molar free energy of Mg_2SiO_4 in the α phase is given by

$$\overline{G}^{\alpha}_{Mg_2SiO_4} = G^{\alpha}_{Mg_2SiO_4}(T) + \int_1^P V^{\alpha}_{Mg_2SiO_4} dP' + RT \ln a^{\alpha}_{Mg_2SiO_4} \quad \text{(A2)}$$

In equation (A2), $G^{\alpha}_{Mg_2SiO_4,T}$ refers to the free energy of pure Mg_2SiO_4 in the α phase at temperature T and 1 bar. Equilibrium between α and β phases gives the conditions

$$\overline{G}^{\beta}_{Mg_2SiO_4} - \overline{G}^{\alpha}_{Mg_2SiO_4} = \Delta G^{\alpha\rightarrow\beta}_{Mg_2SiO_4} = 0$$

$$\overline{G}^{\beta}_{Fe_2SiO_4} - \overline{G}^{\alpha}_{Fe_2SiO_4} = \Delta G^{\alpha\rightarrow\beta}_{Fe_2SiO_4} = 0$$

Upon constructing equations similar to (A2) for the β phase and for the Fe_2SiO_4 components, the above may be expanded to give

$$\Delta G^{\alpha,\beta}_{Mg_2SiO_4} = \Delta G^{\alpha,\beta}_{Mg_2SiO_4}(T) + \int_1^P \Delta V^{\alpha,\beta}_{Mg_2SiO_4} dP' + RT \ln \kappa^{\alpha\rightarrow\beta}_{Mg_2SiO_4} = 0$$

$$\Delta G^{\alpha,\beta}_{Fe_2SiO_4} = \Delta G^{\alpha,\beta}_{Fe_2SiO_4}(T) + \int_1^P \Delta V^{\alpha,\beta}_{Fe_2SiO_4} dP' + RT \ln \kappa^{\alpha\rightarrow\beta}_{Fe_2SiO_4} = 0 \quad \text{(A3)}$$

where the equilibrium constants (the $\kappa_i^{\alpha\rightarrow\beta}$'s) are given by

$$\kappa^{\alpha\rightarrow\beta}_{Mg_2SiO_4} \equiv \frac{a^{\beta}_{Mg_2SiO_4}}{a^{\alpha}_{Mg_2SiO_4}}$$

$$\kappa^{\alpha\rightarrow\beta}_{Fe_2SiO_4} \equiv \frac{a^{\beta}_{Fe_2SiO_4}}{a^{\alpha}_{Fe_2SiO_4}}$$

We may begin by assuming an ideal single-site binary solid solution (i.e., $a_i^{\phi} = X_i^{\phi}$), so that

$$\kappa^{\alpha\rightarrow\beta}_{Mg_2SiO_4} = \frac{X^{\beta}_{Mg_2SiO_4}}{X^{\alpha}_{Mg_2SiO_4}}$$

$$\kappa^{\alpha\rightarrow\beta}_{Fe_2SiO_4} = \frac{X^{\beta}_{Fe_2SiO_4}}{X^{\alpha}_{Fe_2SiO_4}} = \frac{1-X^{\beta}_{Mg_2SiO_4}}{1-X^{\alpha}_{Mg_2SiO_4}}$$

Upon solving these two equations in two unknowns (the $X^{\phi}_{Mg_2SiO_4}$'s), we obtain

$$X^{\alpha}_{Mg_2SiO_4} = \frac{\kappa^{\alpha\beta}_{Fe_2SiO_4} - 1}{\kappa^{\alpha\beta}_{Fe_2SiO_4} - \kappa^{\alpha\beta}_{Mg_2SiO_4}}$$

$$X^{\beta}_{Mg_2SiO_4} = X^{\alpha}_{Mg_2SiO_4} \kappa^{\alpha\beta}_{Mg_2SiO_4} \quad \text{(A4)}$$

We may now solve the two equations (A3) simultaneously for the two unknown equilibrium constants (the $\kappa_i^{\alpha\rightarrow\beta}$'s) and insert these values into equations (A4) to obtain our initial compositional estimate.

This process is easily extended to four equations in four unknowns, for approximation to the solution of the case of univariant equilibrium involving all three phases, by the inclusion of suitable expressions involving $\kappa_i^{\alpha\rightarrow\gamma}$.

APPENDIX B: STEEPEST DESCENT MINIMIZATION

Multicomponent phase equilibria were calculated by a variation of the steepest descent free energy minimization algorithm of *Storey and Van Zeggeren* [1964]. Equilibrium is found at fixed conditions of pressure, temperature, and bulk composition by minimizing the Gibbs free energy G given by

$$G = \sum_{i=1}^{N} \overline{G}_i n_i$$

where $\overline{G}_i$ is the chemical potential of component i in a given phase, n_i is the number of moles of i in the system, and N is the total number of components.

Starting with an initial estimate of the equilibrium values of the n_i, the minimization takes place at constant mass, giving the condition

$$\sum_{i=1}^{N} c_{ji} n_i = m_j \quad \text{(B1)}$$

where m_j is the total number of moles of the jth oxide in the system and c_{ji} is the number of moles of j in the ith component. The free energy is lowered iteratively by introducing a search parameter λ and finding the condition of varying n_i under which the derivative of G with respect to λ is a minimum (i.e., steepest descent). Hence

$$\frac{dG}{d\lambda} = \sum_{i=1}^{N} \overline{G}_i \left(\frac{dn_i}{d\lambda}\right) = \text{minimum} \quad \text{(B2)}$$

It is important to exclude iterative solutions in which the n_i can become negative. This is done by introducing the change of variables

$$n_i = \exp(\eta_i)$$

Thus, from (B1)-(B2) we have

$$\frac{dG}{d\lambda} = \sum_{i=1}^{N} \left(\overline{G}_i n_i\right)\left(\frac{d\eta_i}{d\lambda}\right)$$

with the mass balance conditions

$$\sum_{i=1}^{N} \left(c_{ji} n_i\right)\left(\frac{d\eta_i}{d\lambda}\right) = 0$$

Upon applying an additional normalization condition

$$\sum_{i=1}^{N} \left(\frac{d\eta_i}{d\lambda}\right)^2 = 1 \quad \text{(B3)}$$

the direction of steepest descent is now found by introducing the Lagrange multipiers [cf. *Hurley*, 1980, pp. 223-228] ζ and ξ and so forming the i equations

$$\overline{G}_i n_i - \zeta\left(\frac{d\eta_i}{d\lambda}\right) - \sum_{j=1}^{M} \xi_j c_{ji} n_i = 0 \quad \text{(B4)}$$

where M is the total number of oxide constituents of the system.

Upon multiplying each of these i equations (B4) by $c_{ki}n_i$ and summing over all i, we obtain M simultaneous equations in M unknowns (the ξ_j) such that

$$\sum_{j=1}^{M} \left[\sum_{i=1}^{N} c_{ki} c_{ji} \left(n_i\right)^2\right] \xi_j = \sum_{i=1}^{N} \overline{G}_i c_{ki} \left(n_i\right)^2 \quad \text{(B5)}$$

where $k = 1, \cdots, M$.

Upon solving these equations (B5) for the ξ_j, we obtain the new values of n_i for the next iteration

$$\frac{d\eta_i}{d\lambda} = \frac{n_i}{\varsigma}\left(\overline{G}_i - \sum_{j=1}^{M}\xi_j c_{ji}\right) \quad \text{(B6)}$$

such that

$$\eta_i^{new} = \eta_i^{old} + \left(\frac{d\eta_i}{d\lambda}\right)\Delta\lambda \quad \text{(B7)}$$

where, in equation (B6) above, ς is fixed to satisfy the normalization condition (B3). Note that while the elements of $d\eta_i/d\lambda$ in equation (B7) above determine the direction of steepest descent, a suitable step size $\Delta\lambda$ must be chosen to determine the magnitude of the corrections which are to be made to the composition. We have applied an "accurate line search" algorithm [*Gill et al.*, 1981, pp 100-102] in order to select a step size which will guarantee sufficient descent along the direction of steepest descent. Additionally, we have found it useful to impose the mass balance conditions (B1) at each iteration to minimize the effects of numerical drift.

Acknowledgments. We thank Jim Leven and Hiroshi Sawamoto for kindly providing us with preprints of their respective papers prior to publication, Ray Jeanloz for providing us with experimental data from Kawada (1977), Masaki Akaogi for critical comments on high-pressure experimental data, Don Anderson and Jay Bass for informative discussions on available elasticity and seismic data, and Seth Stein and Emile Okal for helpful discussions of the seismological literature. We also thank Alexandra Navrotsky, Don Anderson, Seth Stein, Jay Bass, and Don Weidner for thoughtful comments on the manuscript. This material is based upon work supported under a National Science Foundation Graduate Fellowship (C.R.B.) and National Science Foundation grant EAR-8416793 (B.J.W.).

REFERENCES

Akaogi, M., and S. Akimoto, High-pressure phase equilibria in a garnet lherzolite, with special reference to Mg^{2+}-Fe^{2+} partitioning among constituent minerals, *Phys. Earth Planet. Inter., 19,* 31-51, 1979.

Akaogi, M., N. L. Ross, P. McMillan, and A. Navrotsky, The Mg_2SiO_4 polymorphs (olivine, modified spinel, and spinel)—Thermodynamic properties from oxide melt solution calorimetry, phase relations, and models of lattice vibrations, *Am. Mineral., 69,* 499-512, 1984.

Akimoto, S., and H. Fujisawa, Olivine-spinel solid solution equilibria in the system Mg_2SiO_4-Fe_2SiO_4, *J. Geophys. Res., 73,* 1467-1479, 1968.

Akimoto, S., T. Yagi, and K. Inoue, High temperature-pressure phase boundaries in silicate systems using in situ x-ray diffraction, in *High Pressure Research—Applications to Geophysics,* edited by M. H. Manghnani and S. Akimoto, pp. 585-602, Academic, Orlando, Fla., 1977.

Anderson, D. L., and J. D. Bass, Mineralogy and composition of the upper mantle, *Geophys. Res. Lett., 11,* 637-640, 1984.

Anderson, D. L., and J. D. Bass, Transition region of the earth's upper mantle, *Nature, 320,* 321-328, 1986.

Anderson, O. L., and R. C. Liebermann, Equations for the elastic constants and their pressure derivatives for three cubic lattices and some geophysical applications, *Phys. Earth Planet. Inter., 3,* 61-85, 1970.

Anderson, O. L., E. Schreiber, R. C. Liebermann, and N. Soga, Some elastic constant data on minerals relevant to geophysics, *Rev. Geophys., 6,* 491-524, 1968.

Ashcroft, N. W., and N. D. Mermin, *Solid State Physics,* 826 pp., Holt, Rinehart and Winston, Philadelphia, Pa., 1976.

Bass, J. D., and D. L. Anderson, Composition of the upper mantle: Geophysical tests of two petrological models, *Geophys. Res. Lett., 11,* 237-240, 1984.

Bernal, J. D., Discussion, *Observatory, 59,* 268, 1936.

Bina, C. R., and B. J. Wood, The eclogite to garnetite transition—Experimental and thermodynamic constraints, *Geophys. Res. Lett., 11,* 955-958, 1984.

Birch, F., Elasticity and constitution of the earth's interior, *J. Geophys. Res., 57,* 227-286, 1952.

Bott, M. H. P., *The Interior of the Earth: Its Structure, Constitution and Evolution,* 403 pp., Elsevier Science, New York, 1982.

Burdick, L. J., and D. V. Helmberger, The upper mantle *P* velocity structure of the western United States, *J. Geophys. Res., 83,* 1699-1712, 1978.

Christensen, U. R., and D. A. Yuen, The interaction of a subducting lithospheric slab with a chemical or phase boundary, *J. Geophys. Res., 89,* 4389-4402, 1984.

Dziewonski, A., and D. L. Anderson, Preliminary reference earth model, *Phys. Earth Planet. Inter., 25,* 297-356, 1981.

Fisher, G. W., and L. G. Medaris, Jr., Cell dimensions and x-ray determinative curve for synthetic Mg-Fe olivines, *Am. Mineral., 54,* 741-753, 1969.

Forsythe, G. E., M. A. Malcolm, and C. B. Moler, *Computer Methods for Mathematical Computations,* 259 pp., Prentice-Hall, Englewood Cliffs, N. J., 1977.

Fyfe, W. S., Hydrothermal synthesis and determination of equilibrium between minerals in the subsolidus region, *J. Geol., 68,* 553-556, 1960.

Gerald, C. F., and P. O. Wheatley, *Applied Numerical Analysis,* 579 pp., Addison-Wesley, Reading, Mass., 1984.

Gill, P. E., W. Murray, and M. H. Wright, *Practical Optimization,* 401 pp., Academic, Orlando, Fla., 1981.

Given, J. W., and D. V. Helmberger, Upper mantle structure of the northwestern Eurasia, *J. Geophys. Res., 85,* 7183-7194, 1980.

Grand, S. P., and D. V. Helmberger, Upper mantle shear structure of North America, *Geophys. J. R. Astron. Soc., 76,* 399-438, 1984.

Hurley, J. F., *Intermediate Calculus: Multivariable Functions and Differential Equations with Applications,* 726 pp., Saunders College, Philadelphia, Pa., 1980.

Ingate, S. F., J. Ha, and K. J. Muirhead, Limitations of waveform modelling of long-period seismograms, *Geophys. J. R. Astron. Soc., 86,* 57-61, 1986.

Jeanloz, R., and A. B. Thompson, Phase transitions and mantle discontinuities, *Rev. Geophys., 21,* 51-74, 1983.

Kawada, K., System Mg_2SiO_4-Fe_2SiO_4 at high pressures and temperatures and the earth's interior, Ph. D. dissertation, Univ. of Tokyo, Tokyo, 1977.

Kennett, B. L. N., The effects of attenuation on seismograms, *Bull. Seismol. Soc. Am., 65,* 1643-1651, 1975.

Lees, A. C., M. S. T. Bukowinski, and R. Jeanloz, Reflection properties of phase transition and compositional change models of the 670 km discontinuity, *J. Geophys. Res., 88,* 8145-8159, 1983.

Leven, J. H., The application of synthetic seismograms to the interpretation of the upper mantle P-wave velocity structure in northern Australia, *Phys. Earth Planet. Inter., 38,* 9-27, 1985.

Liu, L., Phase transformations and the constitution of the deep mantle, in *The Earth: Its Origin, Structure and Evolution,* edited by M. W. McElhinny, pp. 177-202, Academic, Orlando, Fla., 1979.

Muirhead, K., Comments on "Reflection properties of phase transition and compositional change models of the 670-km discontinuity" by Alison C. Lees, M. S. T. Bukowinski, and Raymond Jeanloz, *J. Geophys. Res., 90,* 2057-2059, 1985.

Navrotsky, A., and M. Akaogi, The α, β, γ phase relations in Fe_2SiO_4-Mg_2SiO_4: Calculation from thermochemical data and geophysical applications, *J. Geophys. Res., 89,* 10,135-10,140, 1984.

Nishizawa, O., and S. Akimoto, Partition of magnesium and iron between olivine and spinel, and between pyroxene and spinel, *Contrib. Mineral. Petrol., 41,* 217-230, 1973.

Ringwood, A. E., Phase transformations and the constitution of the mantle, *Phys. Earth Planet. Inter., 3,* 109-155, 1970.

Ringwood, A. E., *Composition and Petrology of the Earth's Mantle,* 618 pp., McGraw-Hill, New York, 1975.

Ringwood, A. E., and A. Major, The system Mg_2SiO_4-Fe_2SiO_4 at high pressures and temperatures, *Phys. Earth Planet. Inter., 3,* 89-108, 1970.

Robie, R. A., B. S. Hemingway, and J. R. Fisher, Thermodynamic properties of minerals and related substances at 298.15 K and 1 bar (10^5 Pa) pressure and at higher temperature, *U.S. Geol. Surv. Bull., 1452,* 456 pp., 1978.

Robie, R. A., C. B. Finch, and B. S. Hemingway, Heat capacity and entropy between 5.1 and 383 Kelvin of fayalite (Fe_2SiO_4): Comparison of calorimetric and equilibrium values for the QFM buffer reaction, *Am. Mineral., 67,* 463-469, 1982.

Sawamoto, H., Single crystal growth of the modified spinel (β) and spinel (γ) phases of $(Mg,Fe)_2SiO_4$ and some geophysical implications, *Phys. Chem. Miner., 13,* 1-10, 1986.

Sawamoto, H., D. Weidner, S. Sasaki, and M. Kumazawa, Single-crystal elastic properties of the modified spinel (beta) phase of magnesium orthosilicate, *Science, 224,* 749-751, 1984.

Silver, P. G., R. W. Carlson, P. Bell, and P. Olson, Mantle structure and dynamics, *Eos Trans. AGU, 66,* 1193-1198, 1985.

Storey, S. H., and F. Van Zeggeren, Computation of chemical equilibrium compositions, *Can. J. Chem. Eng., 42,* 54-55, 1964.

Suito, K., Phase relations of pure Mg_2SiO_4 up to 200 kilobars, in *High Pressure Research—Applications to Geophysics,* edited by M. H. Manghnani and S. Akimoto, pp. 255-266, Academic, Orlando, Fla., 1977.

Sumino, Y., and O. L. Anderson, Elastic constants of minerals, in *CRC Handbook of Physical Properties of Rocks,* Vol. III, edited by R. S. Carmichael, pp. 39-138, CRC Press, Boca Raton, Fla., 1984.

Sumino, Y., O. Nishizawa, T. Goto, I. Ohno, and M. Ozima, Temperature variation of elastic constants of single-crystal forsterite between −190° and 400°C, *J. Phys. Earth, 25,* 377-392, 1977.

Thompson, J. B., Jr., Thermodynamic properties of simple solutions, in *Researches in Geochemistry,* Vol. II, edited by P. H. Abelson, pp. 340-361, John Wiley, New York, 1967.

Verhoogen, J., Phase changes and convection in the earth's mantle, *Philos. Trans. R. Soc. London, Ser. A, 258,* 276-283, 1965.

Walck, M. C., The *P*-wave upper mantle structure beneath an active spreading center: The Gulf of California, *Geophys. J. R. Astron. Soc., 76,* 697-723, 1984.

Watanabe, H., Thermochemical properties of synthetic high pressure compounds relevant to the earth's mantle, in *High Pressure Research in Geophysics,* edited by S. Akimoto and M. H. Manghnani, pp. 441-464, Center for Academic Publications, Tokyo, 1982.

Watt, J. P., G. F. Davies, and R. J. O'Connell, The elastic properties of composite materials, *Rev. Geophys., 14,* 541-563, 1976.

Weidner, D. J., A mineral physics test of a pyrolite mantle, *Geophys. Res. Lett., 12,* 417-420, 1985.

Weidner, D. J., H. Sawamoto, S. Sasaki, and M. Kumazawa, Single-crystal elastic properties of the spinel phase of Mg_2SiO_4, *J. Geophys. Res., 89,* 7852-7860, 1984.

Wood, B. J., and D. G. Fraser, *Elementary Thermodynamics for Geologists,* 303 pp., Oxford University Press, New York, 1977.

Wood, B. J., and J. R. Holloway, Theoretical prediction of phase relationships in planetary mantles, *Proc. Lunar Planet. Sci. Conf. 13th,* Part 1, *J. Geophys. Res., 87,* suppl., A19-A30, 1982.

Wood, B. J., and J. R. Holloway, A thermodynamic model for subsolidus equilibria in the system CaO-MgO-Al_2O_3-SiO_2, *Geochim. Cosmochim. Acta, 48,* 159-176, 1984.

Wood, B. J., and O. J. Kleppa, Thermochemistry of forsterite-fayalite olivine solutions, *Geochim. Cosmochim. Acta, 45,* 529-534, 1981.

Yagi, T., P. M. Bell, and H.-K. Mao, Phase relations in the system MgO–FeO–SiO_2 between 150 and 700 kbar at 1000°C, *Year Book Carnegie Inst. Washington, 78,* 614-618, 1979.

C. R. Bina and B. J. Wood, Department of Geological Sciences, Northwestern University, Locy Hall, Evanston, IL 60201.

(Received April 14, 1986;
revised December 16, 1986;
accepted January 29, 1987.)